Available online at www.sciencedirect.com

ScienceDirect

Mendeleev Commun., 2022, **32**, 83–86

Mendeleev Communications

Near-IR absorbing donor–acceptor charge-transfer gallium complex, an example from non-transition metal chemistry

Arina V. Maleeva,[a] Irina V. Ershova,[a] Olesya Yu. Trofimova,[a] Kseniya V. Arsenyeva,[a] Ilya A. Yakushev[b] and Alexandr V. Piskunov*[a]

[a] *G. A. Razuvaev Institute of Organometallic Chemistry, Russian Academy of Sciences, 603950 Nizhny Novgorod, Russian Federation. E-mail: pial@iomc.ras.ru*

[b] *N. S. Kurnakov Institute of General and Inorganic Chemistry, Russian Academy of Sciences, 119991 Moscow, Russian Federation. E-mail: ilya.yakushev@igic.ras.ru*

DOI: 10.1016/j.mencom.2022.01.027

Gallium(III) catecholates with bipyridine ligand [(3,5-Cat)Ga(bipy)$_2$]I and (3,6-Cat)GaI(bipy) (Cat is di-*tert*-butylcatecholate) were synthesized and characterized by single-crystal X-ray diffraction. The appearance of near-infrared ligand-to-ligand charge transfer for pentacoordinate complex was observed.

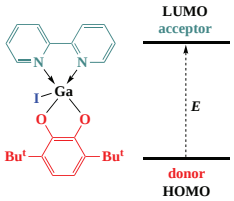

Keywords: gallium, redox-active ligand, catecholate, diimine, X-ray diffraction, electronic spectroscopy.

In the past few decades, a considerable interest in near-infrared (NIR) absorbing compounds has emerged[1] since they can be used in displays and wearable devices,[2] in solar energy conversion schemes and electron-transfer photochemistry, as well as in photovoltaic devices.[3] NIR absorbing materials may include conjugated organic molecules and aggregates,[4] polymers,[5] inorganic materials such as quantum dots,[6] perovskites,[7] and donor–acceptor transition metal complexes.[8–13] The last class of materials is of particular interest due to the large diversity of organic ligands. The straightforward possibility of modernization and combination of the organic donor and acceptor part of such metal derivatives allows fine-tuning of optical properties of resulted compounds.

The relationship between the electronic structure and the energy and intensity of the NIR band in donor–acceptor transition metal (Ni, Pt, Pd, Ru) complexes using redox-active ligands is documented.[13–35] A series of studies deals with intramolecular electron transfer in precious metal complexes between donor (*o*-quinone ligand) and acceptor (fragment with a conjugated system coordinated on the metal), where metal valence orbitals are shifted towards lower or higher energies.[25–35] The HOMO is localized on the *o*-quinone ligand of complexes while the LUMO is localized on the acceptor redox ligand like α-diimine. Due to this modular structure, the electrochemical properties of these complexes can be controlled semi-independently. However, the price of precious metals is a significant disadvantage of their large-scale use. A series of analogous intramolecular redox-active complexes based on nickel was also described.[9,13] A smooth adjustment of the photochemical properties of nickel complexes was demonstrated by varying the donor (catechol) or the acceptor (diamine) parts of complexes.

The localization of photoactive molecular orbitals on the organic fragments in non-transition metal complexes bearing redox-active ligands can provide the appearance of ligand-to-ligand charge transfer (LL'CT). The diversity of non-transition metal complexes with various organic redox-active ligands (*o*-quinones, amidophenolates, diimines) opens up affluent prospects for studying the possible ligand–ligand charge transfer.[36–42] The present paper describes the synthesis of gallium complexes with acceptor bipyridine and donor *o*-benzoquinone ligands and investigation to search for LL'CT.

Gallium catecholate complexes **1** and **2** were obtained one-pot by reacting finely dispersed gallium metal with two *o*-quinones, 3,6-di-*tert*-butyl-*o*-benzoquinone or 3,5-di-*tert*-butyl-*o*-benzoquinone, in THF in the presence of stoichiometric amounts of iodine at 60 °C in the absence of oxygen and air moisture. During the reaction, the solution gradually discolored, which took *ca*. 3 h. The resulting light-colored hot solution was decanted from the metal excess and combined with a hot solution of bipyridine (bipy) in the same solvent. Both reactions were carried out with a molar ratio of organic ligands *o*-quinone/bipy = 1 : 1. However, the elemental analyses of the obtained products have shown that the reaction stoichiometry of gallium

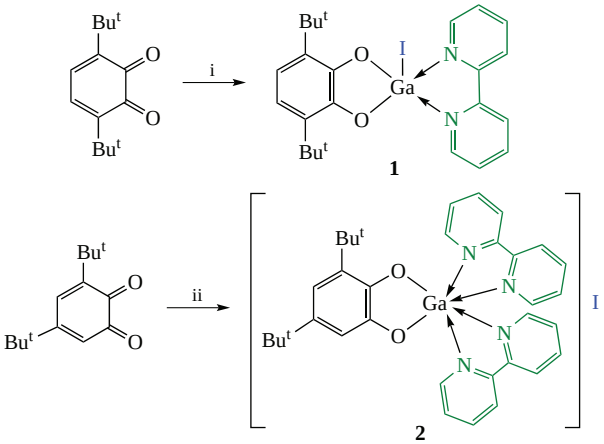

Scheme 1 *Reagents and conditions*: i, Ga (metal), bipy (1 equiv.), I_2 (0.5 equiv.), THF; ii, Ga (metal), bipy (2 equiv.), I_2 (0.5 equiv.), THF.

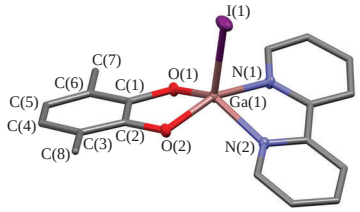

Figure 1 The molecular structure of **1**·PhMe with 30% probability ellipsoids for key atoms. The methyl groups of *tert*-butyls and toluene solvate molecule are omitted for clarity.

derivative with 3,5-di-*tert*-butyl-*o*-benzoquinone (Q/bipy = 1 : 2) is different according to Scheme 1. Such a ratio was used further in the optimized procedure. The gallium catecholates precipitated on slow cooling the reaction mixtures as deep-red (**1**) or orange (**2**) crystalline powders. The crystals suitable for X-ray study were obtained by slow cooling of THF–toluene (for **1**, solvate with PhMe) or THF (for **2**, solvate with four THF molecules) solutions (Figures 1 and 2, respectively).†

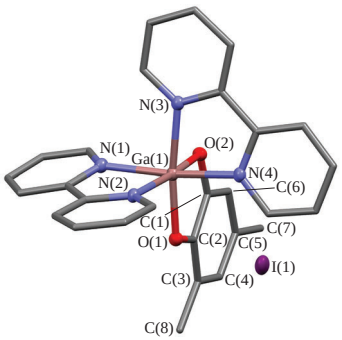

Figure 2 The molecular structure of **2**·$(C_4H_8O)_4$ with 30% probability ellipsoids for key atoms. The methyl groups of *tert*-butyls and four THF solvate molecules are omitted for clarity.

† *Crystal data for* **1**·PhMe. $C_{31}H_{36}GaIN_2O_2$, M = 665.24, orthorhombic, space group *Pbca* at 150(2) K, a = 14.5613(4), b = 18.8824(6) and c = 21.9571(7) Å, Z = 8, V = 6037.2(3) Å^3, d_{calc} = 1.464 g cm^{-3}, $F(000)$ = 2688. A red prism single crystal with dimentions 0.160 × 0.130 × 0.060 mm was selected, and intensities of 90674 reflections were measured using a Bruker D8 Venture Photon single crystal diffractometer [ω- and φ-scan mode, sealed tube Incoatec IμS 3.0, λ(MoKα) = 0.71073 Å, μ = 1.963 mm^{-1}, $2\theta_{max}$ = 58.35°]. After merging of equivalents and absorption correction, 8149 independent reflections (R_{int} = 0.0957) were used for the structure solution and refinement. Final R factors: R_1 = 0.0380 [8149 reflections with $I > 2\sigma(I)$], wR_2 = 0.0653 (all reflections), GOF = 1.013.

Crystal data for **2**·$(C_4H_8O)_4$. $C_{50}H_{68}GaIN_4O_6$, M = 1017.70, triclinic, space group $P\bar{1}$ at 100(2) K, a = 10.1786(9), b = 15.4309(14) and c = 16.5328(15) Å, α = 92.818(3)°, β = 104.567(3)°, γ = 98.870(3)°, Z = 2, V = 2472.7(4) Å^3, d_{calc} = 1.367 g cm^{-3}, $F(000)$ = 1056. An orange prism single crystal with dimentions 0.450 × 0.220 × 0.190 mm was selected, and intensities of 41261 reflections were measured using a Bruker D8 Venture Photon single crystal diffractometer [ω- and φ-scan mode, sealed tube Incoatec IμS 3.0, λ(MoKα) = 0.71073 Å, μ = 1.231 mm^{-1}, $2\theta_{max}$ = 60.068°]. After merging of equivalents and absorption correction, 14421 independent reflections (R_{int} = 0.0386) were used for the structure solution and refinement. Final R factors: R_1 = 0.0399 [14421 reflections with $I > 2\sigma(I)$], wR_2 = 0.1122 (all reflections), GOF = 1.041.

The structures were solved by direct method and refined by full-matrix technique against F^2 in anisotropic approximation. The raw data for both experiments were treated with the APEX3 program suite; experimental intensities were corrected for absorption effects using SADABS program.[43] Molecular graphics was drawn using ChemBioDraw Ultra 14.0.

CCDC 2095157 and 2095158 contain the supplementary crystallographic data for this paper. These data can be obtained free of charge from The Cambridge Crystallographic data Centre *via* http://www.ccdc.cam.ac.uk.

The selected bond lengths and angles for **1**·PhMe and **2**·$(C_4H_8O)_4$ are summarized in Table S1 (see Online Supplementary Materials). The coordination environments of the metal center in these complexes are different. The pentacoordinate metal atom in **1**·PhMe has a distorted square pyramidal environment formed by iodine, two catecholate oxygens, and two bipy nitrogen atoms. The O(1), O(2), N(1), and N(2) atoms form the pyramidal base, while I(1) occupies the apical site in **1**·PhMe. Ionic complex **2**·$(C_4H_8O)_4$ contains hexacoordinate gallium cation and iodide anion. The polyhedron of gallium in cation of **2**·$(C_4H_8O)_4$ is a distorted octahedron formed by the two catecholate oxygen atoms and four nitrogen atoms of two bipy ligands. The O(2), N(1), N(2), and N(4) atoms form the octahedral base, and the O(1) and N(3) atoms occupy the apical sites in **2**·$(C_4H_8O)_4$. The O(1)–Ga(1)–N(3) angle is 172.85(8)°. The Ga–O [1.8687(17)–1.9154(16) Å] and Ga–N [2.054(2)–2.0973(19) Å] bond lengths in **1**·PhMe and **2**·$(C_4H_8O)_4$, and Ga–I bond length [2.5550(4) Å] in **1**·PhMe are typical of gallium catecholates.[44] Note that the C–O bond lengths in **1**·PhMe are slightly shorter than in **2**·$(C_4H_8O)_4$, which may be due to the lower percentage of the coordination sphere filling of the metal center. The distribution of bond lengths in redox-active ligands indicates the dianion character[45] typical of catecholate metal complexes.[44,46] The angle between planes of *o*-quinone ligands and bipy ligands equals 152.77° in **1**·PhMe, 81.05 and 84.49° [for bipy ligand, N(1)–N(2) and N(3)–N(4), respectively] in **2**·$(C_4H_8O)_4$. In both complexes, π–π-staking between the bipy ligands of neighboring molecules is observed [3.487 and 3.536 Å in **1**·PhMe and **2**·$(C_4H_8O)_4$, respectively].

The composition of **1** and **2** in solutions was confirmed by NMR spectroscopy (see Online Supplementary Materials). Redox-active ligand ratios in solutions remains as in crystals. It should be noted that the distortion of the coordination polyhedron from the tetragonal-pyramidal one is preserved in the solution of complex **1**. It is evidenced by the nonequivalence of the protons of the catecholate and bipy ligands in the ^{1}H NMR spectrum.

Several studies of the intensity and arrangement of LL'CT-bands in transition metal complexes depending on the donor–acceptor nature of substituents in organic ligands are presented.[1,13–35] Such dependence should not be expected for **1** and **2** since 3,5- and 3,6-di-*tert*-butylcatecholate ligands are close in their donor ability. The second organic ligand, bipy, is almost unchanged. On the other hand, the geometric differences between complexes **1**, **2** can have a significant effect on their spectroscopic properties. The possibility of an effective intramolecular interaction between orbitals of various organic ligands in the coordination sphere of main-group metal ions is known.[37] The character of such interaction strongly depends on the coordination center structure and the nature of additional substituents.[47–49]

UV/VIS/NIR spectra were recorded for complexes **1** and **2** in MeCN (C = 10^{-3} mol dm^{-3}, Figure 3). It turned out that the band

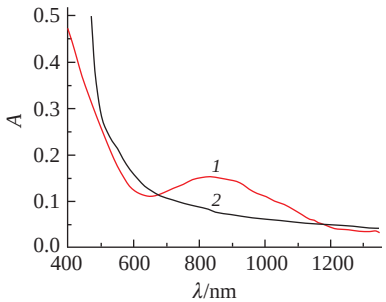

Figure 3 UV/VIS/NIR spectra of complexes (*1*) **1** and (*2*) **2** in MeCN (C = 10^{-3} mol dm^{-3}).

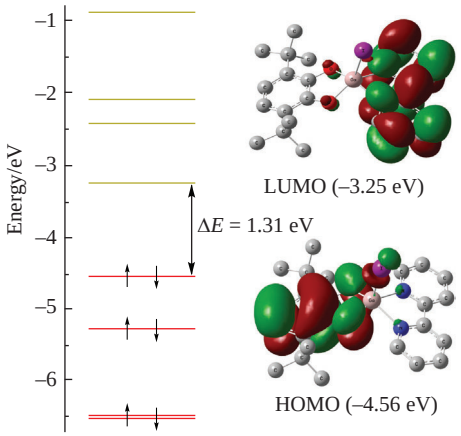

Figure 4 Frontier Kohn–Sham orbital diagram for complex **1** according to DFT calculations at the B3LYP/Def2TZVP level of theory. Isovalue = 0.03 arbitrary units. The H atoms are omitted for clarity.

in the NIR region (λ = 830 nm, $\varepsilon = 1.5 \times 10^2$ dm^3 mol^{-1} cm^{-1}) is observed for compound **1** with a square-pyramidal structure of metal coordination sphere. A similar band for complex **2**·$(C_4H_8O)_4$ with the octahedral environment of metal atom is not so intensive, and only an indistinct wide shoulder is observed in this region of the spectrum.

Density functional theory (DFT) calculations were performed to investigate the electronic structure of gallium complex **1**. The starting experimental (X-ray) geometry of **1** was used to optimize at the B3LYP/Def2TZVP level of theory. The optimized geometry is close to that obtained from the structural experiments. The bond lengths in **1** differ compared to X-ray data by no more than 0.02 Å. The frontier Kohn–Sham orbital diagram with the visualization of frontier orbitals of **1** is presented in Figure 4.

Complex **1** has a well-isolated HOMO (–4.56 eV) orbital located entirely on the catecholate part of complexes with a contribution of iodide p-orbital and a small amount of bipy π-system. The LUMO orbital (–3.25 eV) also has an almost purely ligand nature and occupies the acceptor bipyridine fragment of the complex. However, the halogen and the donor catecholate ligand poorly contribute to this molecular orbital. Thus, complex **1** can be considered as a donor–acceptor compound in which the ligand framework provides electronic properties. The HOMO–LUMO gap determines the long-wavelength peak in the UV/VIS spectrum, corresponding to the ligand–ligand charge transfer (LL'CT). According to calculations, the energy gap between the frontier orbitals in **1** is 1.31 eV. This value is in good agreement with the observed absorption band in the NIR region of the electronic spectrum for **1** (λ = 830 nm, 1.49 eV). Calculated frontier orbitals for the cation of complex **2** are pure ligand in nature. HOMO (–6.75 eV) orbital occupies donor catecholate ligand while two close in energy LUMO (–5.53 eV) and LUMO+1 (–5.45 eV) orbitals are shared between two bipy ligands (for details, see Online Supplementary Materials). HOMO–LUMO gap for complex **2** (1.22 eV) is quite close to the one observed for compound **1**. Still, the octahedral geometry of the complex with 3,5-di-*tert*-butylcatecholate ligand does not promote effective charge transfer between the boundary orbitals. Detailed DFT calculations for these compounds and some related ones will be the subject of the following full paper.

To conclude, the current work demonstrates the ability to construct donor–acceptor chromophores absorbing in VIS/NIR-region based on main group metal complexes with redox-active ligands. The energy of the charge transfer band can be tuned by varying donor and acceptor ligands with different redox properties. The LL'CT intensity can be adjusted within the complex coordination geometry design and selecting additional substituents at the metal atom.

The work was carried out within the framework of the state assignment. The spectroscopy investigations were performed using the equipment of the 'Analytical Center of the IOMC RAS' with the financial support from the grant no. RF-2296.61321X0017 and agreement no. 075-15-2021-670. The single-crystal X-ray diffraction studies were performed using the equipment of the JRC PMR IGIC RAS.

Online Supplementary Materials

Supplementary data associated with this article can be found in the online version at doi: 10.1016/j.mencom.2022.01.027.

References

1 J. A. Weinstein, M. T. Tierney, E. S. Davies, K. Base, A. A. Robeiro and M. W. Grinstaff, *Inorg. Chem.*, 2006, **45**, 4544.
2 O. Ostroverkhova, *Chem. Rev.*, 2016, **116**, 13279.
3 T. M. Clarke and J. R. Durrant, *Chem. Rev.*, 2010, **110**, 6736.
4 X. Lu, S. Lee, Y. Hong, H. Phan, T. Y. Gopalakrishna, T. S. Herng, T. Tanaka, M. E. Sandoval-Salinas, W. Zeng, J. Ding, D. Casanova, A. Osuka, D. Kim and J. Wu, *J. Am. Chem. Soc.*, 2017, **139**, 13173.
5 K. Cai, J. Xie and D. Zhao, *J. Am. Chem. Soc.*, 2014, **136**, 28.
6 Z. Pan, K. Zhao, J. Wang, H. Zhang, Y. Feng and X. Zhong, *ACS Nano*, 2013, **7**, 5215.
7 B.-B. Cui, Y.-W. Zhong and J. Yao, *J. Am. Chem. Soc.*, 2015, **137**, 4058.
8 B.-B. Cui, J.-H. Tang, J. Yao and Y.-W. Zhong, *Angew. Chem., Int. Ed.*, 2015, **54**, 9192.
9 L. A. Cameron, J. W. Ziller and A. F. Heyduk, *Chem. Sci.*, 2016, **7**, 1807.
10 D. Espa, L. Pilia, L. Marchiò, M. L. Mercuri, A. Serpe, E. Sessini and P. Deplano, *Dalton Trans.*, 2013, **42**, 12429.
11 Y. Liu, Z. Zhang, X. Chen, S. Xu and S. Cao, *Dyes Pigm.*, 2016, **128**, 179.
12 J. L. Wong, R. F. Higgins, I. Bhowmick, D. X. Cao, G. Szigethy, J. W. Ziller, M. P. Shores and A. F. Heyduk, *Chem. Sci.*, 2016, **7**, 1594.
13 W. W. Kramer, L. A. Cameron, R. A. Zarkesh, J. W. Ziller and A. F. Heyduk, *Inorg. Chem.*, 2014, **53**, 8825.
14 T. J. Dunn, L. Chiang, C. F. Ramogida, K. Hazin, M. I. Webb, M. J. Katz and T. Storr, *Chem. – Eur. J.*, 2013, **19**, 9606.
15 R. M. Clarke, K. Hazin, J. R. Thompson, D. Savard, K. E. Prosser and T. Storr, *Inorg. Chem.*, 2016, **55**, 762.
16 L. Chiang, A. Kochem, O. Jarjayes, T. J. Dunn, H. Vezin, M. Sakaguchi, T. Ogura, M. Orio, Y. Shimazaki, F. Thomas and T. Storr, *Chem. – Eur. J.*, 2012, **18**, 14117.
17 L. Chiang, K. Herasymchuk, F. Thomas and T. Storr, *Inorg. Chem.*, 2015, **54**, 5970.
18 L. Lecarme, L. Chiang, J. Moutet, N. Leconte, C. Philouze, O. Jarjayes, T. Storr and F. Thomas, *Dalton Trans.*, 2016, **45**, 16325.
19 T. Storr, E. C. Wasinger, R. C. Pratt and T. D. P. Stack, *Angew. Chem., Int. Ed.*, 2007, **46**, 5198.
20 T. Kurahashi and H. Fujii, *J. Am. Chem. Soc.*, 2011, **133**, 8307.
21 S. Aono, M. Nakagaki, T. Kurahashi, H. Fujii and S. Sakaki, *J. Chem. Theory Comput.*, 2014, **10**, 1062.
22 T. Kurahashi and H. Fujii, *Inorg. Chem.*, 2013, **52**, 3908.
23 A. Kochem, G. Gellon, N. Leconte, B. Baptiste, C. Philouze, O. Jarjayes, M. Orio and F. Thomas, *Chem. – Eur. J.*, 2013, **19**, 16707.
24 R. M. Clarke, T. Jeen, S. Rigo, J. R. Thompson, L. G. Kaake, F. Thomas and T. Storr, *Chem. Sci.*, 2018, **9**, 1610.
25 N. M. Shavaleev, E. S. Davies, H. Adams, J. Best and J. A. Weinstein, *Inorg. Chem.*, 2008, **47**, 1532.
26 J. Yang, D. K. Kersi, L. J. Giles, B. W. Stein, C. Feng, C. R. Tichnell, D. A. Shultz and M. L. Kirk, *Inorg. Chem.*, 2014, **53**, 4791.
27 M. D. Ward, *J. Solid State Electrochem.*, 2005, **9**, 778.
28 P. A. Scattergood, P. Jesus, H. Adams, M. Delor, I. Sazanovich, H. D. Burrows, C. Serpa and J. A. Weinstein, *Dalton Trans.*, 2015, **44**, 11705.
29 R. Roy, P. Chattopadhyay and C. Sinha, *Polyhedron*, 1996, **15**, 3361.
30 G. K. Rauth, S. Pal, D. Das, C. Sinha, A. M. Z. Slawin and J. D. Woollins, *Polyhedron*, 2001, **20**, 363.
31 K. Tahara, T. Kadowaki, J. Kikuchi, Y. Ozawa, S. Yoshimoto and M. Abe, *Bull. Chem. Soc. Jpn.*, 2018, **91**, 1630.
32 S. Sobottka, M. Nößler, A. L. Osterichter, G. Hermann, N. Z. Subat, J. Beerhues, M. van der Meer, L. Suntrup, U. Albold, S. Hohloch, J. Tremblay and B. Sarkar, *Chem. – Eur. J.*, 2020, **26**, 1314.

33 K. Heinze and S. Reinhardt, *Chem. – Eur. J.*, 2008, **14**, 9482.
34 N. Deibel, D. Schweinfurth, J. Fiedler, S. Záliš and B. Sarkar, *Dalton Trans.*, 2011, **40**, 9925.
35 J. Best, I. V. Sazanovich, H. Adams, R. D. Bennett, E. S. Davies, A. J. H. M. Meijer, M. Towrie, S. A. Tikhomirov, O. V. Bouganov, M. D. Ward and J. A. Weinstein, *Inorg. Chem.*, 2010, **49**, 10041.
36 I. V. Ershova and A. V. Piskunov, *Russ. J. Coord. Chem.*, 2020, **46**, 154 (*Koord. Khim*., 2020, **46**, 132).
37 I. V. Ershova, A. V. Piskunov and V. K. Cherkasov, *Russ. Chem. Rev.*, 2020, **89**, 1157.
38 A. I. Poddel'sky, V. K. Cherkasov and G. A. Abakumov, *Coord. Chem. Rev.*, 2009, **253**, 291.
39 A. Raghavan and A. Venugopal, *J. Coord. Chem.*, 2014, **67**, 2530.
40 K. V. Tsys, M. G. Chegerev, G. K. Fukin, A. G. Starikov and A. V. Piskunov, *Mendeleev Commun.*, 2020, **30**, 205.
41 A. A. Skatova, N. L. Bazyakina, I. L. Fedushkin, A. V. Piskunov, N. O. Druzhkov and A. V. Cherkasov, *Russ. Chem. Bull., Int. Ed*., 2019, **68**, 275 (*Izv. Akad. Nauk., Ser. Khim*., 2019, 275).
42 I. N. Meshcheryakova, K. V. Arsenyeva, G. K. Fukin, V. K. Cherkasov and A. V. Piskunov, *Mendeleev Commun.*, 2020, **30**, 592.
43 G. M. Sheldrick, *Acta Crystallogr.*, 2015, **C71**, 3.
44 A. V. Piskunov, A. V. Maleeva, I. N. Mescheryakova and G. K. Fukin, *Eur. J. Inorg. Chem.*, 2012, 4318.
45 S. S. Batsanov, *Russ. J. Inorg. Chem.*, 1991, **36**, 1694 (*Zh. Neorg. Khim*., 1991, **36**, 3015).
46 M. G. Chegerev, A. V. Piskunov, A. V. Maleeva, G. K. Fukin and G. A. Abakumov, *Eur. J. Inorg. Chem.*, 2016, 3813.
47 A. V. Piskunov, I. V. Ershova, A. S. Bogomyakov, A. G. Starikov, G. K. Fukin and V. K. Cherkasov, *Inorg. Chem.*, 2015, **54**, 6090.
48 I. V. Ershova, A. S. Bogomyakov, G. K. Fukin and A. V. Piskunov, *Eur. J. Inorg. Chem.*, 2019, 938.
49 A. V. Piskunov, I. N. Meshcheryakova, M. S. Piskunova, N. V. Somov, A. S. Bogomyakov and S. P. Kubrin, *J. Mol. Struct.*, 2019, **1195**, 417.

Received: 9th July 2021; Com. 21/6610